

Supplementary Information

Stabilizing sodium metal battery with synergy effects of sodiophilic matrix and fluorine-rich interface

Qidi Wang^{a,b}, Chenglong Zhao^c, Xiaohui Lv^{a,b}, Yaxiang Lu^c, Kui Lin^{a,b}, Shaoqiong Zhang^{a,b}, Feiyu Kang^{a,b}, Yong-Sheng Hu^{c,}, and Baohua Li^{a,b,d,*}*

^aDivision of Energy and Environment, Engineering Laboratory for the Next Generation Power and Energy Storage Batteries, Graduate School at Shenzhen, Tsinghua University, Shenzhen 518055, China

^bSchool of Materials Science and Engineering, Tsinghua University, Beijing 100084, China

^cKey Laboratory for Renewable Energy, Beijing Key Laboratory for New Energy Materials and Devices, Beijing National Laboratory for Condensed Matter Physics, Institute of Physics, Chinese Academy of Sciences, Beijing 100190, China

^dShenzhen Geim Graphene Research Center, Shenzhen 518055, China

E-mail: libh@mail.sz.tsinghua.edu.cn, yshu@aphy.iphy.ac.cn

Experimental Section

Composite anode fabrication.

The Na-carbon composite electrode (NCCE) was prepared by a facial molten Na infusion method using hydrophilic carbon cloth from CeTech. The employed carbon matrix was punched into 10 mm discs and pre-heated at 1200 °C for 4 h in a tubular furnace under an argon flow and then naturally cooled down to room temperature. After the heat treatment, carbon cloth was directly transport into an Ar-filled glovebox to prevent any moisture exposition. The fabrication of NCCE was operated in the glovebox with less than 0.5 ppm O₂ and H₂O. Fresh solid Na cube (99.9%, Alfa Aesar) was put into a nickel crucible and heated to 300 °C to get molten Na. After that, the carbon matrix was partially put into liquefied Na, and as can be seen in the **Movie S1** (Supporting Information), molten Na instantly infuse into the whole carbon cloth, forming NCCE after cooling down to room temperature.

Sample synthesis.

Na₃V₂(PO₄)₃ cathode was prepared by a solid-state reaction. A stoichiometric ratio (1:1) of sodium carbonate (Na₂CO₃), ammonium dihydrogen phosphate (NH₄H₂PO₄) was dissolved in the deionized water with continuous stirring from a clear solution A. While stoichiometric vanadium (III) acetylacetonate (VO(C₅H₇O₂)₂) was dissolved in ethyl alcohol with continuous stirring from a clear solution or suspension B. The stoichiometric ratio of Na₂CO₃, NH₄H₂PO₄ and VO(C₅H₇O₂)₂ is 3:2:3. Then, adding the solution A into the B by dropping with continuous stirring for overnight at room temperature in order to obtain a homogenous suspension. After that, the suspension liquid was left loosely covered at 80 °C until the liquid was evaporated, and the obtain

mixture was heated at 300 °C for 10 h in Ar/H₂ (90:10). Then mixture was thoroughly mixed and ground in an agate mortar and further heated in Ar atmosphere at 800 °C for 12 hours with an intermediate grinding and cooled to room temperature naturally. After the heat treatment, the material was directly put into an Ar-filled glovebox to prevent any moisture exposition.

Characterizations.

The morphology of the materials was investigated using a scanning electron microscope (SEM) (Hitachi SU-8010). Raman spectra was collected on a Horiba LabRAM HR800 spectrometer with a 532nm laser. Nitrogen adsorption/desorption isotherms were measured on an ASAP2020M+C apparatus at 77 K, and specific surface area and pore diameter distribution were determined by the Brunauer-Emmett-Teller (BET) and Barrett-Joyner-Halenda (BJH) methods, respectively. Powder X-ray diffraction (XRD) was performed using a Bruker D8 Advance diffractometer equipped with a Cu K radiation source ($\lambda_1=1.54060 \text{ \AA}$, $\lambda_2=1.54439 \text{ \AA}$) and a LynxEye XE-T detector. Rietveld refinement of the XRD analysis was carried out using the General structure analysis system (GSAS) software.^[1] The X-ray photoelectron spectra (XPS) of the samples were performed on PHI 5000 VersaProbe II spectrometer using monochromatic Al K(alpha) X-ray source calibrated with respect to carbon (284.8 eV). Operando optical microscopy images were conducted in glovebox at ambient temperature in dark field, using an Olympus BXFM microscope with a CCD camera in combine with a Land 2001A battery testing system. Symmetrical cells were assembled inside an argon-filled

glove box. The area of the Na anode is around 0.3 cm^2 and the current applied is $300 \text{ }\mu\text{A}$ with each charge/discharge time of 0.5 h.

Electrochemical measurement.

2032-type coin cells were assembled with two identical electrodes, which were either NCCE or bare Na foils. The cathode electrodes used in full cells were prepared via mixing 70 wt % active material with 20 wt % super P and 10 wt % polyvinylidene fluoride (PVDF) and on Al foil, and punched into 10 mm discs with the loading mass of the active material was $\sim 9 \text{ mg cm}^{-2}$. The prepared electrodes were dried at $120 \text{ }^\circ\text{C}$ under vacuum for 10 h and then were fabricated into CR2032 coin-type full cells with either pure sodium foil or NCCE as the coupling anode electrode. All batteries were assembled in an argon-filled glovebox (H_2O , $\text{O}_2 < 0.1 \text{ ppm}$) using the dose of electrolyte (100-120 μL), and glass fiber A was used as the separator. 1 M NaPF_6 in FEC/DMC (1:1 v/v) and EC/DMC (1:1 v/v) are used as the experimental group and the control group, respectively. Battery-grade NaPF_6 was purchased from Shanshan Corporation Ltd. Before use, the NaPF_6 salt was dried for 2 days under vacuum at $100 \text{ }^\circ\text{C}$. Dimethyl carbonate (DMC), ethylene carbonate (EC) and fluoroethylene carbonate (FEC), were bought from Sigma-Aldrich Industrial Corporation. The charge and discharge measurements were carried out on a Land 2001A battery testing system at 25°C . The long cycling performance comparisons of $\text{Na} \parallel \text{Na}_3\text{V}_2(\text{PO}_4)_3$ full cells using either NCCE or bare Na as the anode were cycled in galvanostatic mode with first three cycles at 0.2C (23.4 mA g^{-1}) and the following cycles at 3.0C (351 mA g^{-1}) with a voltage range of 2.0-4.0 V. The $\text{Na} \parallel \text{Na}_3\text{V}_2(\text{PO}_4)_3$ full cells for rate performance were cycled

with a voltage range of 2.0-4.0 V at the rate from 0.1C to 15C. Electrochemical impedance spectroscopy was carried out on the Solartron 1470E multichannel electrochemical station in the frequency range of 0.1 Hz–1 MHz with a potential amplitude of 10 mV .

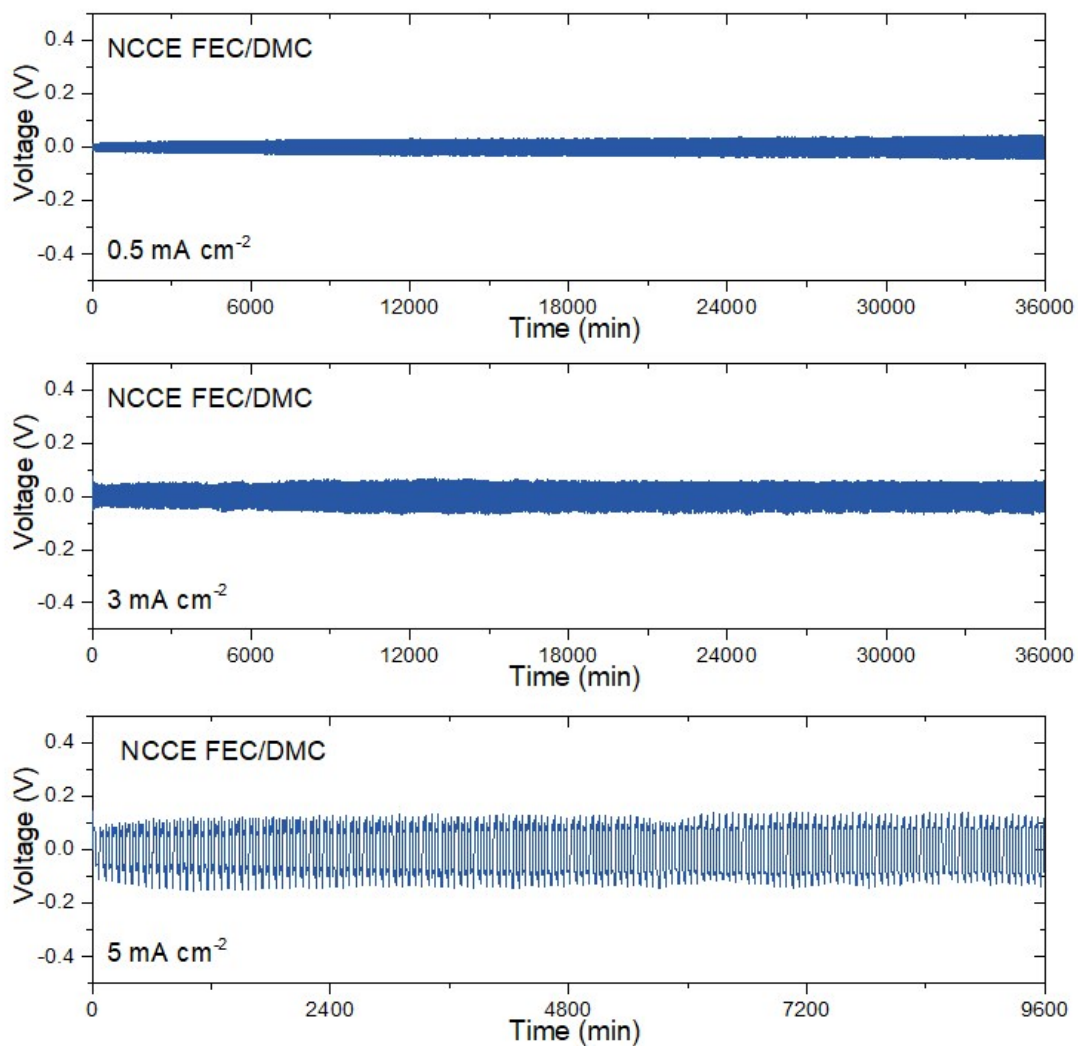


Figure S1. Galvanostatic plating-stripping profiles of NCCE symmetric cell at a current density of 0.5 mA cm^{-2} , 3.0 mA cm^{-2} and 5.0 mA cm^{-2} for 0.5 h.

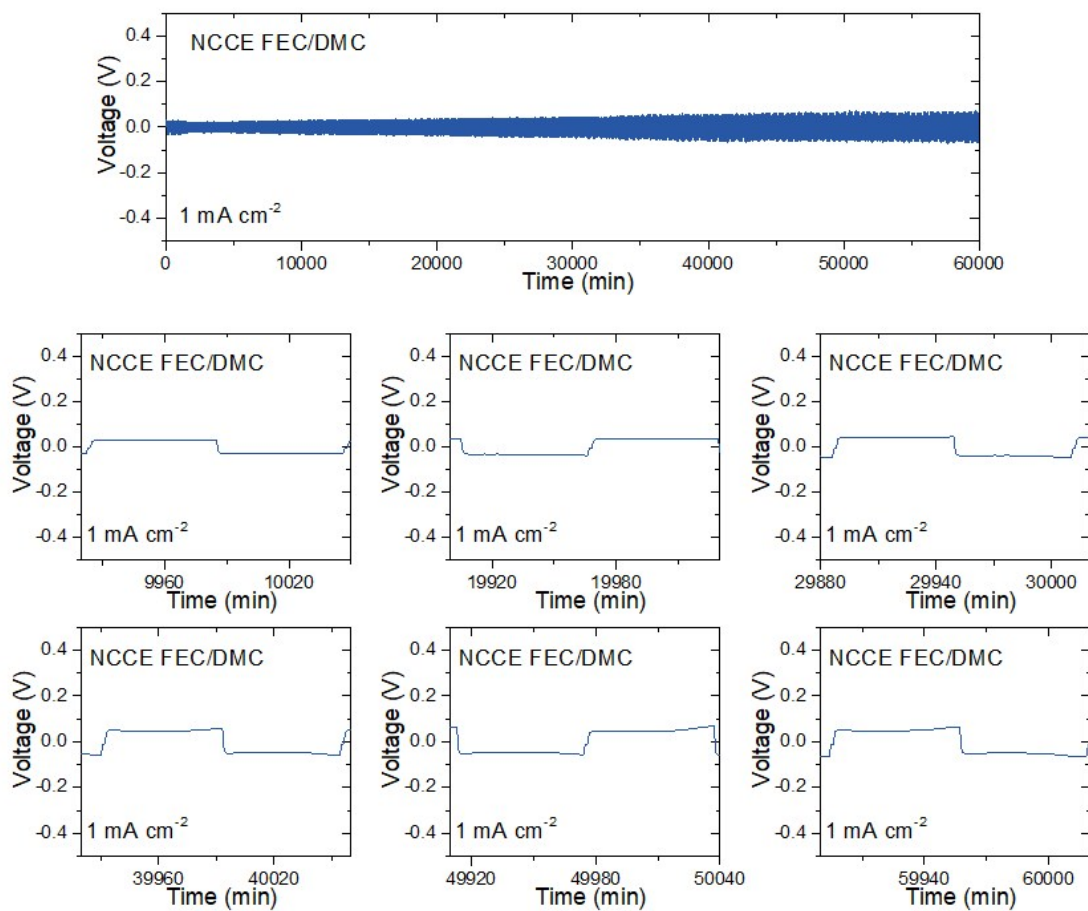


Figure S2. Galvanostatic plating-stripping profiles of NCCE symmetric cell at a current density of 1.0 mA cm^{-2} for 1 h. Magnified voltage profiles of batteries after various cycles.



Figure S3. Digital photographs of commercial carbon matrix.

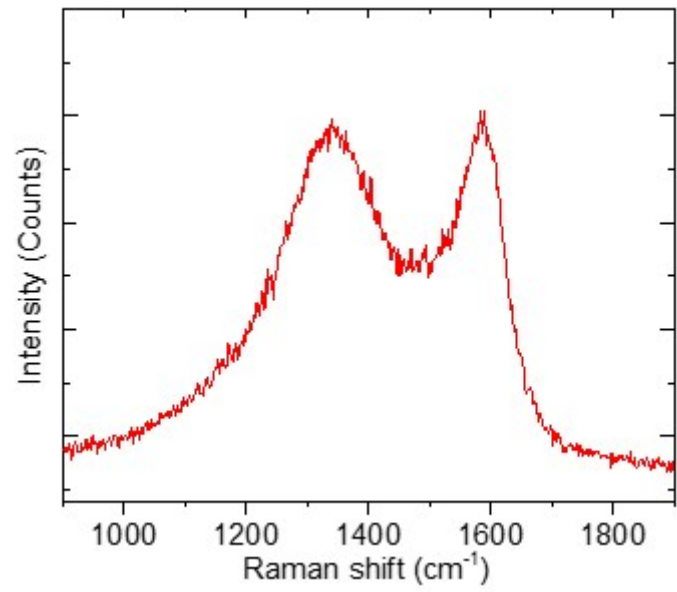


Figure S4. Raman spectra of carbon matrix after heat treatment.

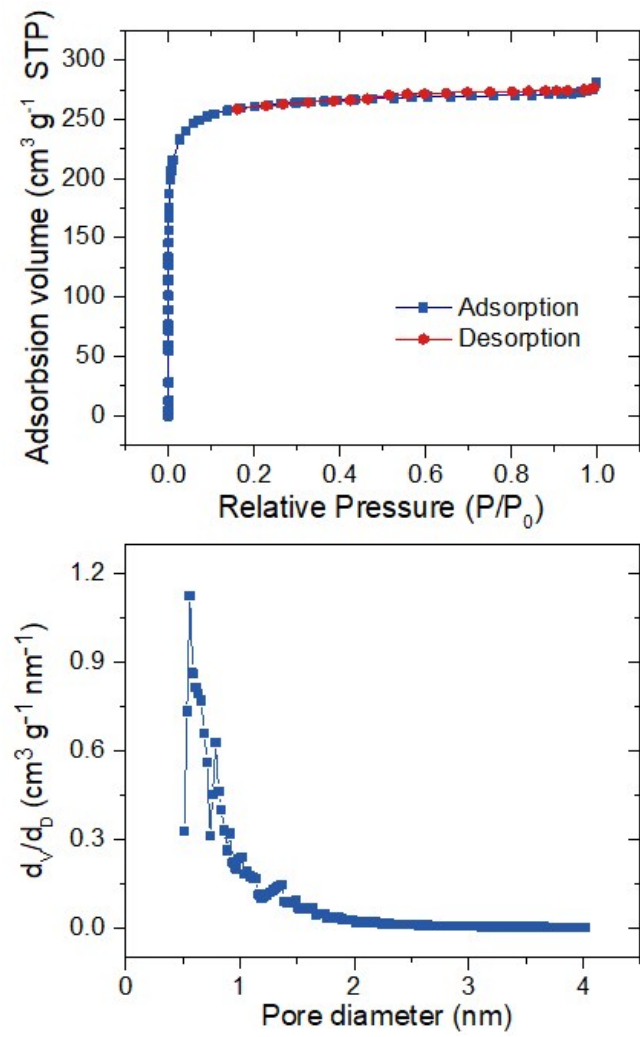


Figure S5. Nitrogen adsorption-desorption isotherm and pore size distribution of carbon matrix.

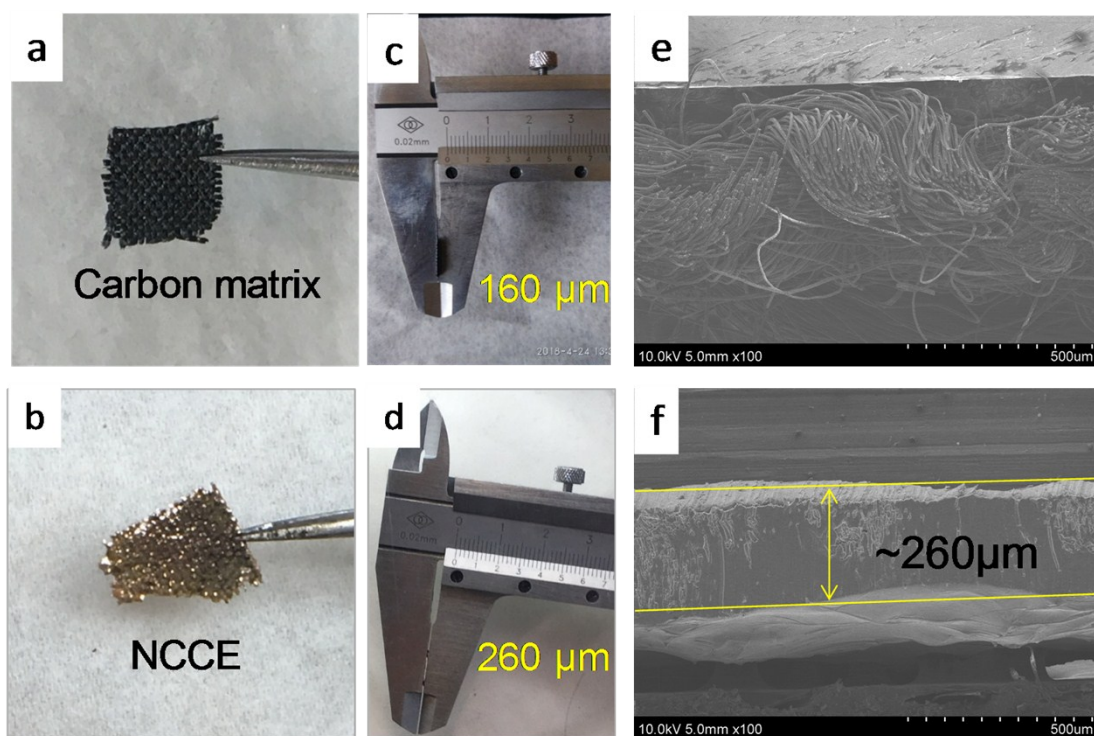


Figure S6. (a, b) Digital photographs and thickness measurements of carbon matrix and NCCE by Vernier caliper (c, d) and SEM images (e, f).

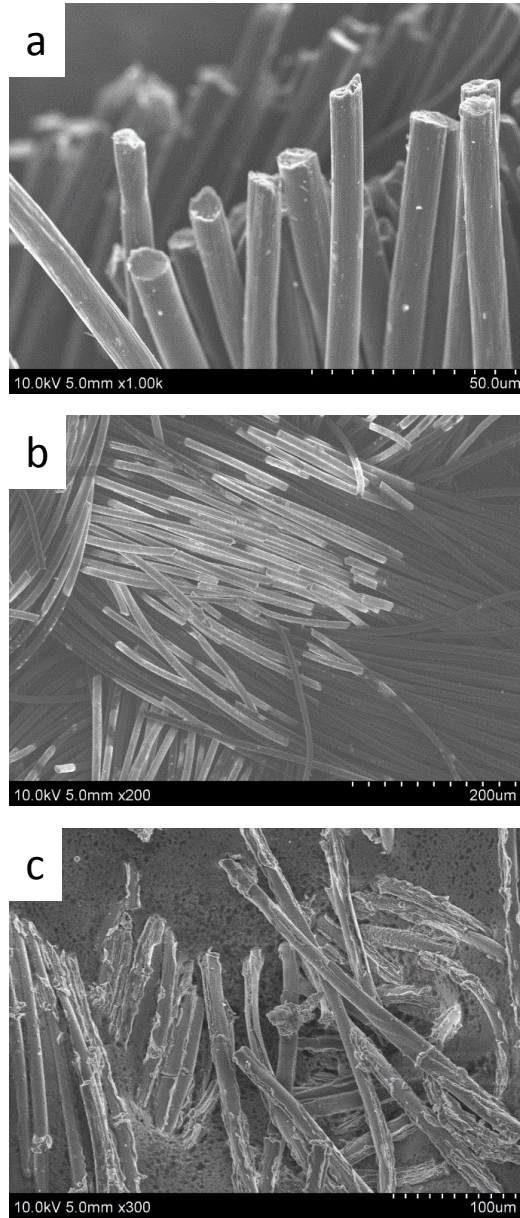


Figure S7. SEM images of carbon matrix with different Na-infusion process (a-c).

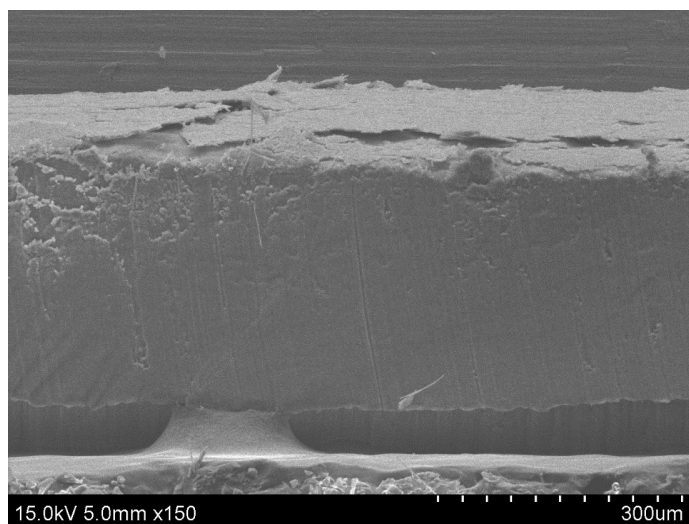


Figure S8. The cross-section SEM image of the bare Na electrode after 50 cycles.

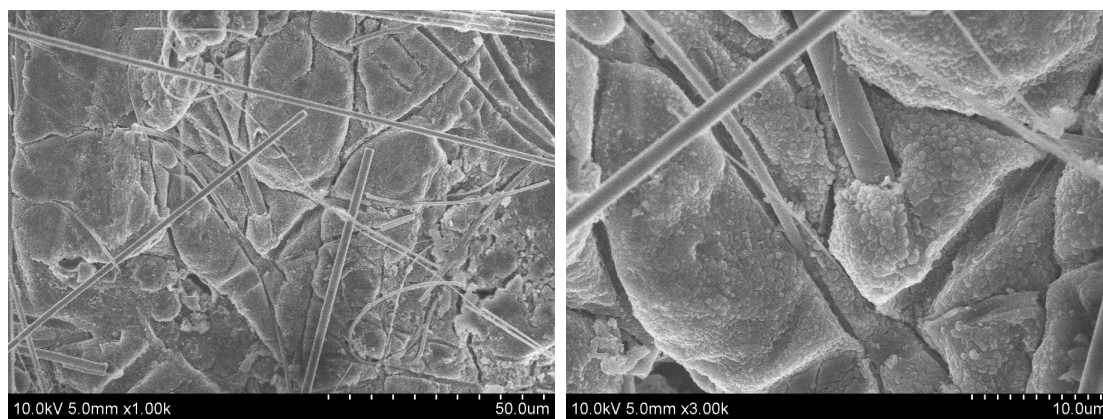


Figure S9. Morphology of the NCCE in FEC/DMC electrolyte at different current densities at a current density of 3 mA cm^{-2} for 0.5 h after 50 cycles. The fibers scattering on the surface is the residual fragments of the glass fiber separator.

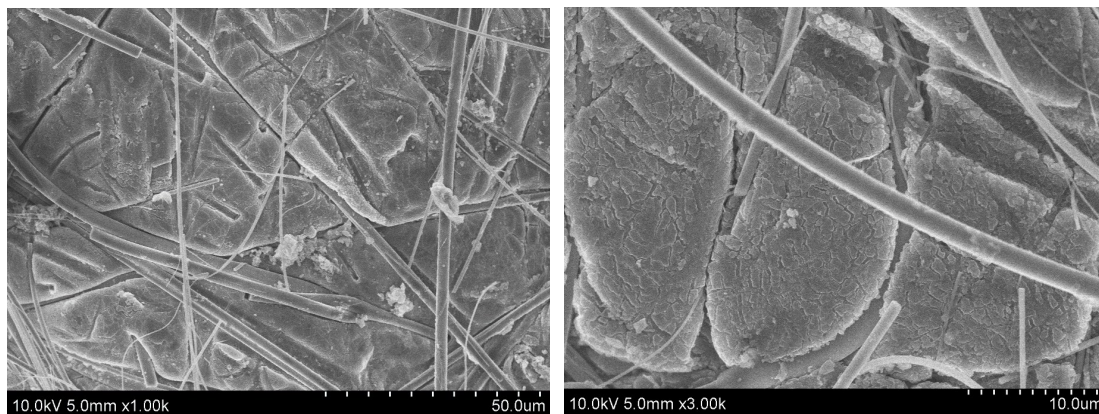


Figure S10. Morphology of the NCCE in FEC/DMC electrolyte at different current densities at a current density of 5 mA cm^{-2} for 0.5 h after 50 cycles.

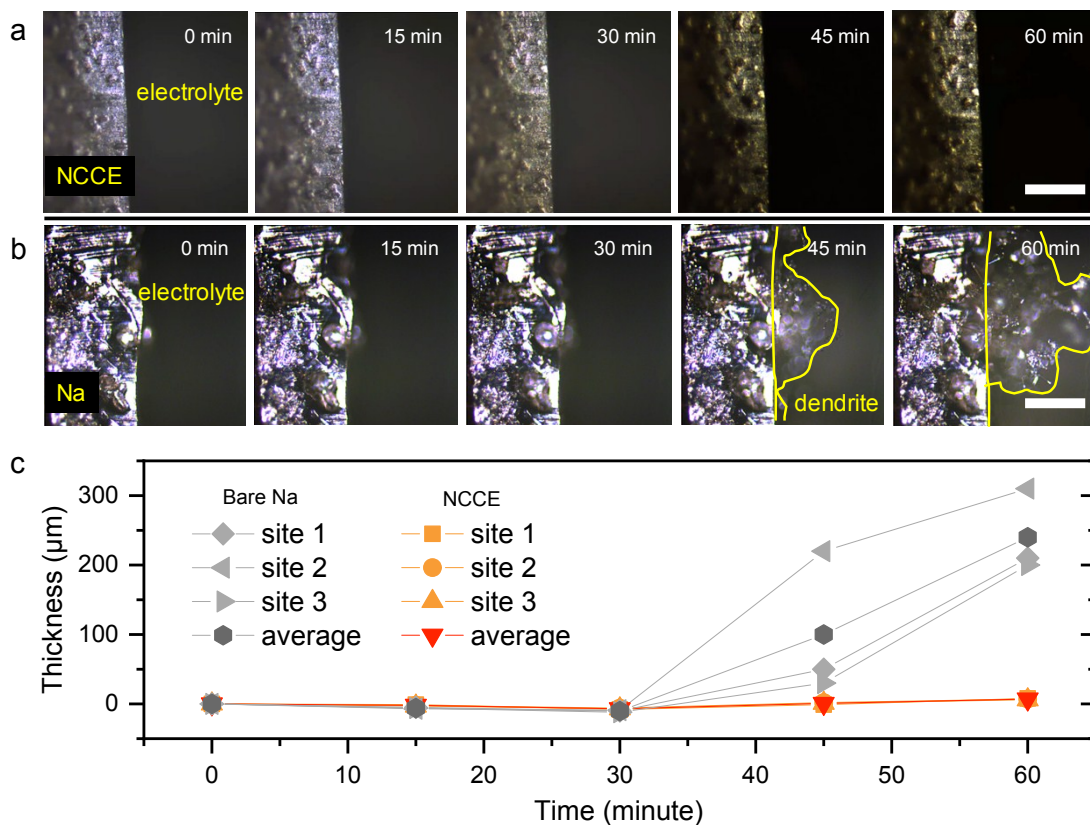


Figure S11. *Operando* optical microscopy images of two electrodes. Cross-section images of NCCE (a) and bare Na (b) symmetric cells recorded at 0 min, 15 min, 30 min, 45 min and 60 min respectively. The scale bar in both (a) and (b) are 200 μm . (c) The evolution of the Na metal deposit thickness during plating and stripping. Three sampling locations, at 1/4, 1/2 and 3/4 top down along the Na-metal foil, are chosen to measure the changes in thickness, from which the average thickness is calculated.

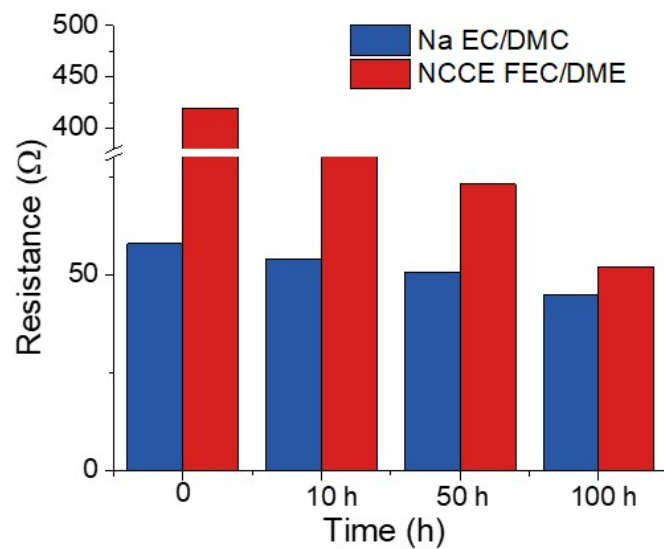


Figure S12. Impedance spectra of NCCE and bare Na symmetric cells after 0 h, 10 h, 50 h, and 100 h at a current density of 0.5 mA cm^{-2} for 0.5 h.

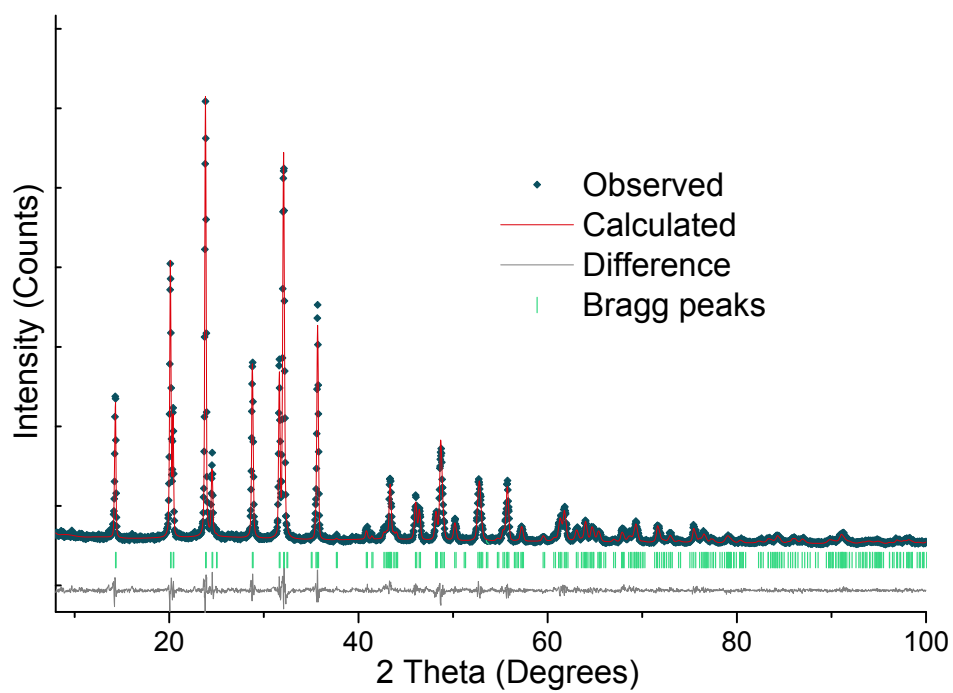


Figure S13. Rietveld refinement of high-resolution XRD pattern of $\text{Na}_3\text{V}_2(\text{PO}_4)_3$.

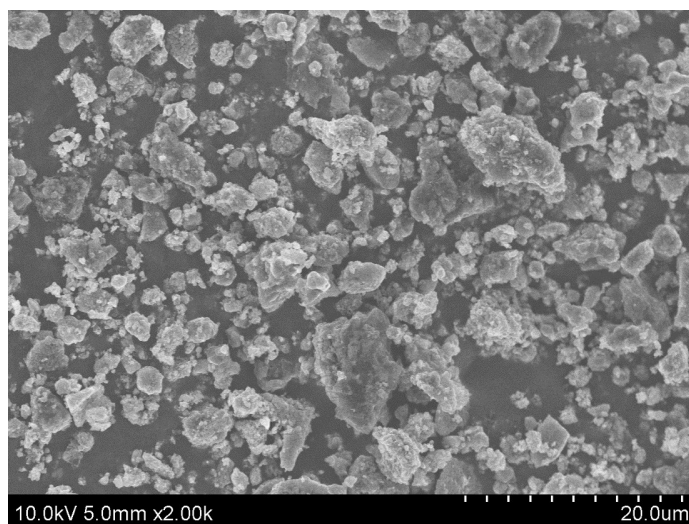


Figure S14. SEM image of as-prepared Na₃V₂(PO₄)₃ cathode.

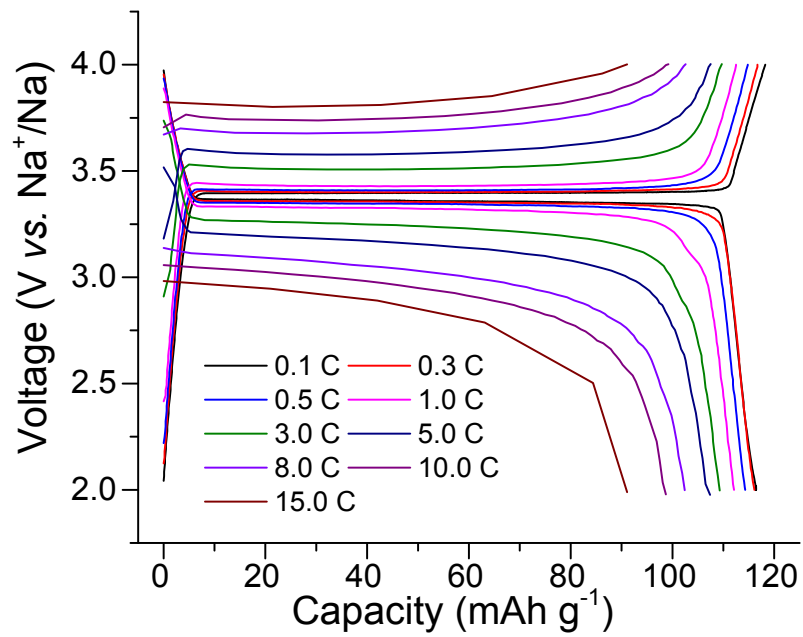


Figure S15. Galvanostatic charge-discharge voltage profiles of NCCE-NaVPO full cell at different current densities.

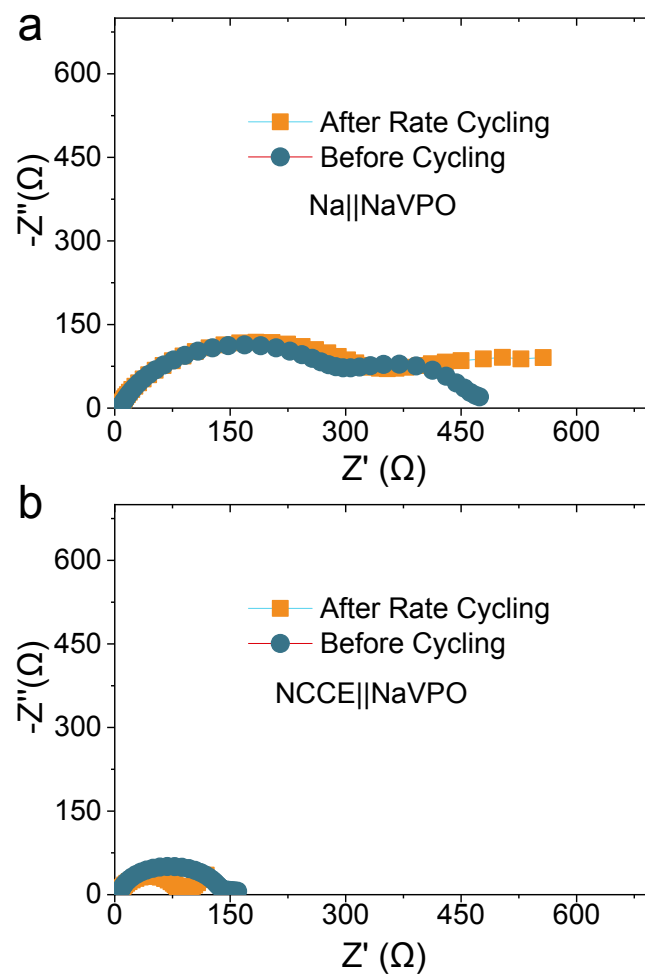


Figure S16. Nyquist plot of the impedance spectra of the (a) bare Na and (b) NCCE full cell before and after cycles.

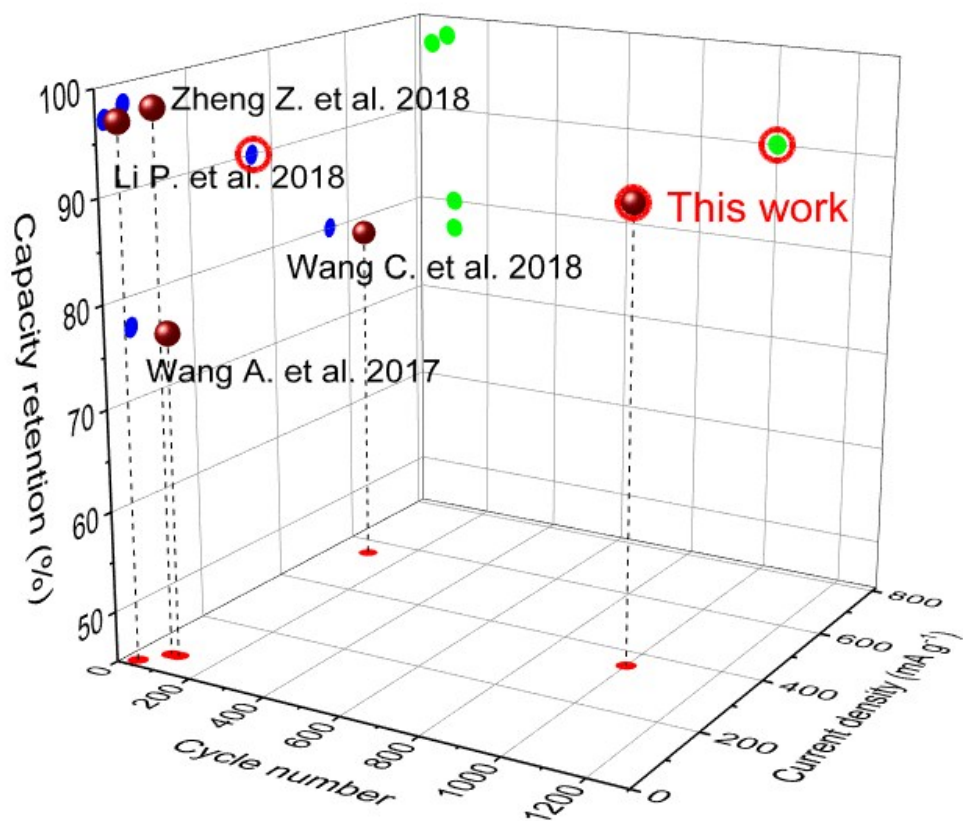


Figure S17. Comparison of the full-cell performance with NaVPO as cathode and various kinds of Na metal anodes. See Table S6 for the detail.

Table S1. Comparison of short circuit time using different electrolytes and electrodes.

Electrode Electrolyte	NCCE	bare Na
	1M NaPF ₆ FEC/DMC	>36000 min
1M NaPF ₆ EC/DMC	8250 min	5600 min

Table S2. Summary of the reported literature on nanostructured hosts for Na metal anodes in Na-Na cell.

Host materials for Na metal anode	electrolyte	Current density (mA cm ⁻²)	Capacity limit (mAh cm ⁻²)	Cycle time (h)	ref
		0.5	0.25	600	
Sodiophilic carbon matrix	1M NaPF₆ in FEC/DMC	1	0.5	600	This work
		1	1	1000	
		3	1.5	600	
		5	5	160	
RGO	1M NaClO ₄ in EC/PC	0.5	0.125	60	[2]
	1 M NaPF ₆ in DGME	1	1	600	
Na@CP-NCNTs	1 M NaPF ₆ in EC/PC	1	1	350	[3]
		3	1	180	
		5	3	90	
Carbon felt	1 M NaClO ₄ in EC/PC	1	2	480	[4]
S-Cu matrix	1 M NaClO ₄ in EC/DEC	0.5	1	200	[5]
		1	1	100	
O-Cu matrix	1 M NaClO ₄ in EC/DEC	0.5	1	400	[5]
		1	1	200	
SnO ₂ -CF	1M NaClO ₄ in EC/DMC/EMC	0.5	1	300	[6]
MoS ₂	1 M NaClO ₄ in EC/DEC with 10% FEC	0.5	0.25	100	[7]

Table S3. The concentration of the element of SEI of NCCE and bare Na anode from the XPS results.

Element	Atomic %	
	NCCE	bare Na anode
Na1s	24.29	18.35
O1s	38.03	42.02
F1s	8.68	3.12
C1s	28.89	29.36
P2p	0.12	7.15

Table S4. Crystallographic and Rietveld refinement data of $\text{Na}_3\text{V}_2(\text{PO}_4)_3$.

Space group	$R\text{-}3c$ (167) - Rhombohedral
Wavelengths	1.5406 Å
Cell parameters	$a = b = 8.73223(33)$ Å,
	$c = 21.8369(12)$ Å
	$\alpha = \beta = 90^\circ, \gamma = 120^\circ$
	$V = 1442.02(15)$ Å ³ , $Z = 6$
Reliability factors	$R_{wp} = 6.43\%$
	$R_p = 4.81\%$
	$Gof = 1.745$
	$R(F^2) = 2.94$

Table S5. Atomic coordinates, occupancies and isotropic displacement parameters (\AA^2) of $\text{Na}_3\text{V}_2(\text{PO}_4)_3$ compound.

	x	y	z	Occupancy	U_{iso}	Wyckoff
Na1	1/3	2/3	1/6	0.704(26)	0.159(15)	6b
Na2	2/3	0.9678(12)	1/12	0.790(15)	0.084(7)	18e
V	1/3	2/3	0.01911(14)	1.0	1.0	12
P	-0.0426(5)	1/3	1/12	1.0	0.028(4)	18
O1	0.1397(7)	0.4982(7)	0.0791(4)	1.0	0.026(5)	36
O2	0.5421(8)	0.8464(7)	-0.02553(28)	1.0	0.045(5)	36

Table S6. Summary of the reported literature of Na₃V₂(PO₄)₃-Na anode full cells

Modified strategies	electrolyte	loading mass of active materials (mg cm ⁻²)	Current density (mA g ⁻¹)	Initial capacity (mAh g ⁻¹)	Capacity (mAh g ⁻¹) (Capacity retention)	ref
Anode host	1M NaPF₆ in FEC/DMC	9	351	112	101(1000 cycles, 90%)	This work
Anode host	1 M NaClO ₄ in EC/PC	2	59	110	85(100 cycles, 77%)	[2]
Anode host	1 M NaClO ₄ in EC/DEC	1	550	100	~80(100 cycles, 80%)	[5]
Anode host	1M NaPF ₆ in DEGDME	4–5	59	97	95(80 cycles, 98%)	[5]
Anode host	1 M NaClO ₄ in PC with 5vol% FEC	8.6	~18.6	108	~104(35 cycles, 97%)	[9]
Polymer protective Layer	1 M NaClO ₄ in EC/PC	-	100	120	97(160 cycles, 81%)	[10]

Note 1: The calculation of the practical capacity.

The composite anode has a diameter of 10mm containing an average Na loading of 51.05 mg and the carbon cloth host of 5.25 mg, resulting in the areal loading of Na metal of 65mg cm⁻². Weight percentage of Na in the NCCE is 90.7%, and the corresponding gravimetric specific capacity is $1166 \text{ mAh g}^{-1} \times 90.7\% \approx 1057.5 \text{ mAh g}^{-1}$.^[4]

References

1. C. Larson and R. B. Von Dreele, General structure analysis system (GSAS). Los Alamos National Laboratory Report LAUR 2004, 86, 748.
2. Wang, A., et al., *Processable and Moldable Sodium-Metal Anodes*. *Angewandte Chemie*, 2017. **129**(39): p. 12083-12088.
3. Zhao, Y., et al., *High Capacity, Dendrite-Free Growth, and Minimum Volume Change Na Metal Anode*. *Small*, 2018. **14**(20): p. 1703717.
4. Chi, S.-S., et al., *3D Flexible Carbon Felt Host for Highly Stable Sodium Metal Anodes*. *Advanced Energy Materials*, 2018. **8**(15): p. 1702764.
5. Wang, C., et al., *A Chemically Engineered Porous Copper Matrix with Cylindrical Core-Shell Skeleton as a Stable Host for Metallic Sodium Anodes*. *Advanced Functional Materials*, 2018. **28**(30): p. 1802282.
6. Zhang, Y., et al., *3D Wettable Framework for Dendrite-Free Alkali Metal Anodes*. *Advanced Energy Materials*, 2018. **8**(18): p. 1800635.
7. Zhang, D., et al., *Simultaneous Formation of Artificial SEI Film and 3D Host for Stable Metallic Sodium Anodes*. *ACS Applied Materials & Interfaces*, 2017. **9**(46): p. 40265-40272.
8. Zheng, Z.-J., et al., *Nitrogen and Oxygen Co-Doped Graphitized Carbon Fibers with Rich-Sodiophilic Sites Guide Uniform Sodium Nucleation for Ultrahigh Capacity Sodium Metal Anodes*. *ACS Applied Materials & Interfaces*, 2018.
9. Li, P., et al., *Highly reversible Na and K metal anodes enabled by carbon paper protection*. *Energy Storage Materials*, 2018. **15**: p. 8-13.
10. Wei, S., et al., *Highly Stable Sodium Batteries Enabled by Functional Ionic Polymer Membranes*. *Advanced Materials*, 2017. **29**(12): p. 1605512.